Available online at www.sciencedirect.com
ScienceDirect
Scripta Materialia 60 (2009) 1141–1144
Scripta MATERIALIA
www.elsevier.com/locate/scriptamat

Nanoprecipitate-hardened 1.5 GPa steels with unexpected high ductility

D. Raabe,* D. Ponge, O. Dmitrieva and B. Sander

Max-Planck-Institut für Eisenforschung, Max-Planck-Str. 1, 40237 Düsseldorf, Germany

Received 27 January 2009; revised 28 February 2009; accepted 28 February 2009
Available online 9 March 2009

We present mechanical and microstructure results on precipitation-hardened ductile high-strength martensitic and austenitic–martensitic steels (up to 1.5 GPa strength) with good ductility. The alloys have a low-carbon content (0.01 wt.% C), 9–12 wt.% Mn, and minor additions of Ni, Ti and Mo (1–2 wt.%). Hardening is based on transformation-induced plasticity and the formation of intermetallic nanoprecipitates in the martensite during heat treatment (aging). The approach leads to an unexpected simultaneous increase in both strength and total elongation.

Keywords: Steel; High strength; Aging; Precipitation; Intermetallic

Steels with very high strength above 1 GPa and good ductility (total elongation of 15–20% in tensile testing) are future key materials for lightweight engineering solutions and corresponding CO_2 savings [1–5] (Fig. 1).

We present surprising results on low-alloyed materials that were developed by combining the transformation-induced plasticity (TRIP) effect with the martensite aging (maraging) effect. The TRIP mechanism exploits the deformation-stimulated transformation of unstable austenite into martensite and the resulting plasticity required to accommodate the transformation misfit [3–10]. The maraging effect uses the hardening of the heavily strained martensite through the formation of nanosized intermetallic precipitates. These precipitations act as highly efficient obstacles to dislocation motion thereby enhancing the strength of the material [11–16].

While both types of alloys, i.e. TRIP steels [3–10] and maraging steels [11–16], have been investigated in some depth, the combination of the two mechanisms has not yet received much attention.

The combination of the TRIP and maraging concepts in one alloy is alone sufficient to justify a detailed study as it promises an approach to enhance the strength of conventional steels without the use of large quantities of expensive alloying elements. Unfortunately, the downside of this approach is that the increase in strength is usually accompanied by a drop in ductility (quantified here in terms of the total elongation) (Fig. 1). However, surprisingly, the opposite trend is observed in the present case: we observed the simultaneous increase in strength and ductility upon formation of nanoscaled precipitates.

The materials studied combine different hardening mechanisms. The first one is the formation of strain-induced martensite (alloys with 0.01 wt.% C and 12 wt.% Mn have retained austenite fractions up to 15 vol.%) and exploits the same hardening principles as TRIP steels [3–10]. The second one is the strain hardening of the ductile low carbon α'- and ε-martensite and of the remaining retained austenite. The third one is the formation of nanosized intermetallic precipitates in the martensite during heat treatment (i.e. maraging). These precipitates are highly dispersed owing to the favorable nucleation conditions in the heavily strained martensite matrix in which they form.

The steels show not only excellent mechanical properties but also an unexpected relationship between strength and total elongation as both quantities increase upon aging. In addition to the optimization of yield strength, ultimate tensile strength and elongation to fracture, we also are trying to make a material that is characterized by homogeneous strain hardening.

Here we report results for a 9 wt.% Mn and a 12 wt.% Mn alloy (9Mn: 8.86 wt.% Mn, 0.0065 wt.% C, 2.0 wt.% Ni, 1.07 wt.% Mo, 1.04 wt.% Ti, 0.047 wt.% Si, 0.086 wt.% Al; 12Mn: 11.9 wt.% Mn, 0.0101 wt.% C, 2.06 wt.% Ni, 1.12 wt.% Mo, 1.09 wt.% Ti, 0.057 wt.% Si, 0.116 wt.% Al). Both alloys have a very low-carbon

* Corresponding author. Tel.: +49 211 6792 340; fax: +49 211 6792 279; e-mail: d.raabe@mpie.de

1359-6462/$ - see front matter © 2009 Acta Materialia Inc. Published by Elsevier Ltd. All rights reserved.
doi:10.1016/j.scriptamat.2009.02.062

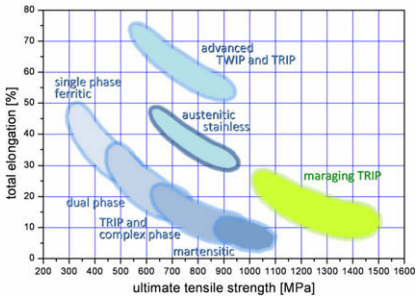

Figure 1. Typical strength–ductility profiles of steels. The data represent regimes such as published in the references given below. TRIP: transformation-induced plasticity; TWIP: twinning-induced plasticity; maraging TRIP: steel concept which uses hardening mechanisms based on transformation-induced plasticity and the formation of intermetallic nanoprecipitates in the martensite during heat treatment (aging).

content and minor additions of Ni, Ti and Mo which are required to form the nanoprecipitates. The difference among the samples consists in their Mn content (~9 wt.%, ~12 wt.%), and hence in the amount of retained austenite.

The alloys were melted and cast to round billets of 1 kg in a vacuum induction furnace. Annealing and swaging was conducted to ensure homogenization and removal of segregation. After annealing at 1150 °C for 1 h, swaging was conducted in eight passes between 1000 and 1150 °C (true strain of 1.39). This was followed by air cooling to 800 °C and a water quench to room temperature. The rods were reheated to 1100 °C for 0.5 h, hot rolled in six passes (true strain of 1.9) and water quenched. These strips were cold rolled to a thickness of 1.5 mm (true strain of 1). The subsequent solution heat treatment was performed at 1050 °C for 0.5 h followed by water quench. Final aging was conducted at different temperatures between 425 and 500 °C at times between 1 min and 48 h. Tensile testing was conducted on a Zwick ZH 100 using strain gage extensometer at a constant cross-head velocity corresponding to an initial strain rate of 8×10^{-4} s^{-1}.

Characterization was conducted using optical and scanning electron microscopy (SEM) in conjunction with energy-dispersive X-ray spectrometry (EDX) and high-resolution electron back scatter diffraction (EBSD). SEM was performed using a JEOL JSM-6500F field emission scanning electron microscope operated at 15 kV. The EBSD scans were carried out in areas of about 100×270 μm^2 in cross-sections in the middle of the samples at a step size of 500 nm.

Transmission electron microscopy (TEM) images were taken of a solution-treated, quenched plus finally age-hardened sample with 12 wt.% Mn in order to study the size and spatial distribution of the nanoprecipitates which are formed during aging. For TEM sample preparation the material was first thinned to a thickness below 100 μm by mechanical polishing. Standard 3 mm TEM discs were then punched and electropolished into TEM thin foils using a Struers Tenupol twin-jet electropolishing device. The electrolyte consisted of 5% perchloric acid ($HClO_4$) in 95% ethanol cooled to −30 °C. The thinned specimens were investigated in a JEOL JEM 2200 FS field emission transmission electron microscope operated at 200 kV. The analysis was carried out in scanning TEM mode (STEM) using a bright-field (BF) detector (BF-STEM).

Figure 2a shows the engineering stress–strain curves of the age-hardenable Mn steel with 9 wt.% Mn. The EBSD analysis reveals coarse α′-martensite lamellae of up to 100 μm in length, but no retained austenite appears in the solution-annealed and quenched state. This means that it is not an age-hardenable TRIP steel but a Mn-based maraging steel. Its yield strength (YS) is about 350 MPa, its ultimate tensile strength (UTS) about 810 MPa, and the total elongation (TE) about 6% in the as-quenched state. The properties of the same material after heat treatment (48 h at 450 °C) are surprising. The UTS is above 1 GPa while the TE does not drop upon precipitation strengthening as observed for conventional Ni–Co-based maraging steels [11–15] but it increases from 6% to more than 15%. This means that aging in this martensitic alloy simultaneously increases both strength and ductility. 15% pre-deformation (by cold rolling) of the same sample prior to the same aging procedure (Fig. 2a) yields similar properties as without pre-deformation. This result is plausible as the material did not contain instable austenite, hence no TRIP effect occurs.

A similar observation is made for the 12 wt.% Mn alloy (Fig. 2b). This sample has also an α′-martensite matrix but it contains up to 15 vol.% retained austenite and some ε-martensite. Hence, the 12 wt.% Mn alloy represents an age-hardenable TRIP steel (we refer to it as a maraging TRIP steel) as it can undergo hardening via deformation-induced martensite formation and via martensite hardening through precipitates.

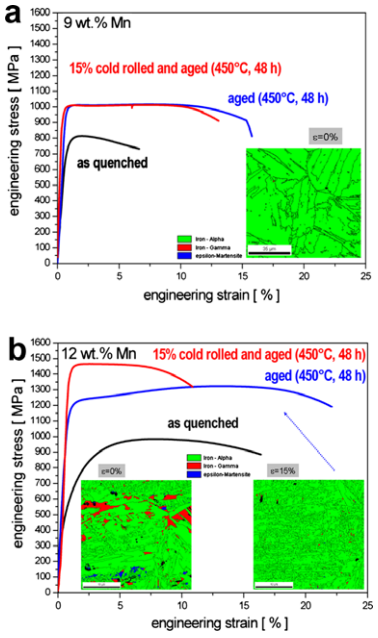

Figure 2. Stress–strain curves for the two Fe–Mn alloys. The 9 wt.% Mn alloy (a) has no retained austenite. The 12 wt.% Mn alloy (b) has up to 15 vol.% retained austenite prior to deformation which is gradually reduced during straining. Both alloys show the unexpected effect that the ultimate tensile strength and the total elongation simultaneously increase upon aging heat treatment (450 °C, 48 h).

The EBSD map shows a finer α′-martensite microstructure than in the 9 wt.% Mn sample. Dilatometry (measurement of thermal expansion) and ferromagnetic data suggest in part a higher austenite fraction of up to 20 vol.%. The differences between dilatometry, ferromagnetic characterization and EBSD can be attributed to the limited statistics provided by EBSD. Also EBSD yields surface information only. The size of the retained austenite islands lies between 1 and 20 μm. The ε-martensite lamellae are below 2 μm and occupy an overall fraction of about 1–2 vol.%.

The sample has a YS of about 325 MPa, UTS of nearly 1 GPa, and TE of about 16% in the as-quenched state. After aging heat treatment (450 °C for 48 h) the UTS increases to more than 1.3 GPa and the TE to 21%. 15% cold rolling prior to aging leads to a strong increase in strength (nearly 1.5 GPa UTS) but also to a drop in TE (about 10%). The increase in strength is attributed to the deformation-stimulated transformation of the retained austenite leading to a TRIP effect and, to a lesser extent, to the assumed higher dispersion of the precipitates formed under improved nucleation conditions in the deformation-induced martensite. The motivation for attributing the additional strain-hardening capacity of the 12 wt.% Mn alloy not only to the precipitates but also to the occurrence of the TRIP effect becomes clear when considering the following observations.

First, comparison of the flow curve of the 9 wt.% Mn sample with that of the 12 wt.% Mn sample for the 15 wt.% pre-rolled state reveals that the 12 wt.% Mn sample (containing retained austenite) shows a strong increase in strength while the 9 wt.% sample (no retained austenite) does not reveal any change in strength upon 15% cold rolling prior to testing (Fig. 2a and b). Second, an additional EBSD analysis conducted after 15% straining for the 12 wt.% Mn sample (EBSD phase map in Fig. 2b) shows that the retained austenite has vanished. This result was confirmed by magnetic measurements. Third, we measured the martensite start temperature for both alloys by dilatometry and also calculated it using the empirical equation of Hossein Nedjad et al. [17]. The dilatometry experiment showed a martensite start temperature of $T_{Ms} = 294$ °C for the 9 wt.% Mn alloy (150 °C according to the equation [17]) and of $T_{Ms} = 70$ °C for the 12 wt.% Mn alloy (25 °C according to the equation [17]).

Regarding the ductility, it is remarkable that both steels show, irrespective of their retained austenite content, the surprising feature of a simultaneous increase in both UTS and total elongation upon aging. While the UTS increases by 25–30% the total elongation increases by more than 150% (from 6% to 15%) for the 9 wt.% Mn sample and by 31% (from 16% to 21%) for the 12 wt.% Mn alloy. This increase of both properties represents a very unusual feature of these materials.

The BF-STEM micrographs that were taken of the age-hardened TRIP steel (12 wt.% Mn) show that the nanoscaled precipitates have a narrow size distribution with an average diameter of 8–12 nm (Fig. 3a–c). Local EDX analysis conducted in convergent beam mode shows an increased content in Ni, Ti and Al in these precipitates when compared to the surrounding matrix. This observation raised the possibility that these small precipitates might be γ′ phase, $Ni_3(Ti,Al)$ according to results on Ni–Co-based maraging steels alloyed with Ti and Mo [12,13,18]. The area density of the nanoprecipitates was about 300 μm^{-2}. The volume density is estimated as $5 \times 10^3\ \mu m^{-3}$ (about 2–3 vol.%). Slightly elongated nanoprecipitates are located at the interfaces between the lamellae. These precipitates are about twice as long as those inside the grains (Fig. 3b). Besides these tiny precipitates, larger ones were also observed in the 12 wt.% Mn sample. They had an average size of 1–2 μm. EDX revealed that these precipitates contained Ti, Mo, C and Al.

The TEM data hence reveal that the steels, like conventional maraging steels, contain nanosized precipitates that are very highly dispersed, even after long heat treatments. The observation of a high maintained strength and a strong tendency for the nanoscaled precipitates not to coarsen has been reported previously for conventional maraging steels [14]. Using an Orowan line tension approximation for dislocation bow-out between the nanoprecipitates (10 nm diameter) and an average precipitate spacing of about 100 nm suggests an increase in yield strength upon aging of about 350 MPa. This increase in strength roughly matches the change in yield strength observed.

In addition to the nanoprecipitates, the dislocation content in the martensite matrix is also important for the strength. For example, Figure 3c shows that the dislocation density in the martensite was about 10^{15}–$10^{16}\ m^{-2}$. It is noteworthy that the dense dislocation arrangement prevailed even after the aging treatment. The dislocation density could also play an important role in the nucleation of the precipitates and their very high dispersion. Figure 3c shows that many precipitates are located at dislocations. It is also important for the plastic properties that the (nearly) carbon-free martensite matrix is rather duc-

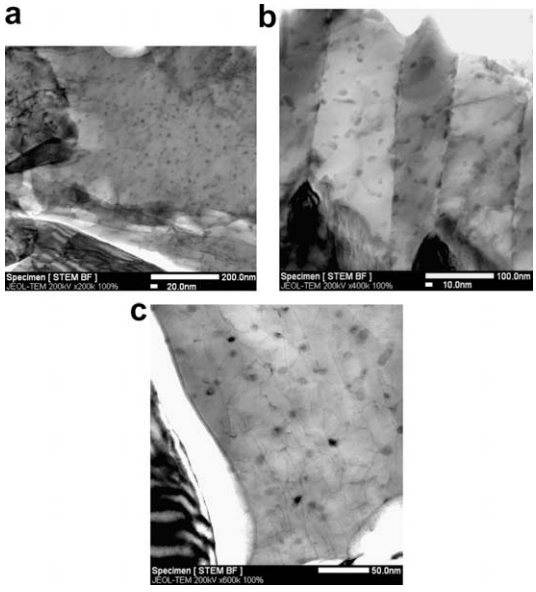

Figure 3. TEM images of nanoprecipitates formed in the aged 12 wt.% Mn alloy (500 °C, 2 h). The precipitates have an average diameter of 8–12 nm. Local EDX analysis shows an increased content in Ni, Ti and Al in the precipitates relative to the matrix. We speculate that they might be γ′ phase precipitates, $Ni_3(Ti,Al)$.

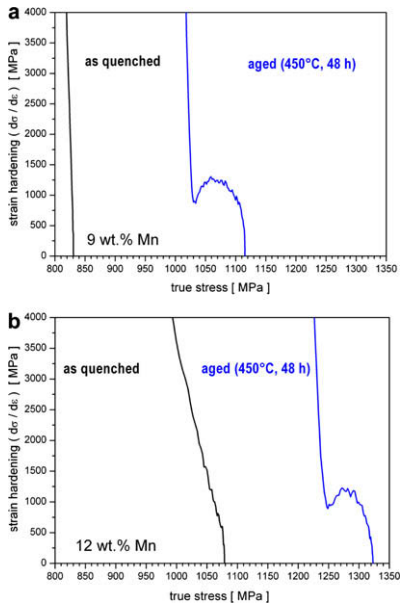

Figure 4. Kocks–Mecking analysis (strain hardening vs. stress curve) of the two alloys. Aging leads to a second hardening level at large stresses which does not appear in the as-quenched specimens. We interpret this effect in terms of Orowan hardening.

tile. Conventional carbon-based martensitic steels typically reveal very poor ductility (Fig. 1).

A central point of the current observations is the unexpected strong increase in the total elongation after aging (Fig. 2). Two effects are conceivable to explain this phenomenon: first, the kinetics associated with delayed austenitization; and second, the kinetics of precipitation.

Regarding austenitization, it has been observed in conventional maraging steels that the heating rate and the holding times both influence the kinetics of retransformation from martensite to austenite [19]. In other words it is conceivable that very long heat treatment times (450 °C, 48 h) entail delayed austenitization. Dilatometry studies at different heating rates confirm this phenomenon. Our data show the first deviation in length expansion from martensite upon reheating at a temperature of about 550 °C for the 12 wt.% Mn sample when using a quite rapid heating rate of 0.86 K s^{-1}. The same experiment conducted at a heating rate of 0.086 K s^{-1} revealed a lower transformation point from martensite into austenite at around 500 °C. Thermodynamic predictions also suggest a transformation around 480 °C although some of the data underlying such simulations for Mn-containing Fe-based multicomponent systems are not considered as very reliable.

These findings initially seem to indicate that partial retransformation into austenite might play a role in the observed ductilization, at least for the specimen with 12 wt.% Mn. On the other hand, the alloy with only 9 wt.% Mn shows the same ductilization effect although retransformation at 450 °C is thermodynamically most unlikely for this alloy owing to its low austenite-stabilizing Mn content (Fig. 2b).

A more plausible explanation for the ductilization effect can be seen in the Orowan hardening mechanism that starts to set in at a stress of about 1030 MPa (Fig. 4). The Kocks–Mecking analysis (strain hardening vs. stress curve) shows that this hardening effect is not active at the beginning of the tensile test. The second hardening plateau can also not be attributed to the TRIP effect as this mechanism occurs in both the 9 and 12 wt.% Mn samples after heat treatment.

In addition, the Kocks–Mecking curves for the as-quenched samples (not heat treated, hence no aging) (Fig. 4) do not show a second hardening plateau. A corresponding analysis on conventional Ni–Co-based maraging steel does not show this effect either. This means that the second hardening plateau can be attributed to Orowan hardening. The reason that this mechanism does not occur at the beginning of straining is attributed to the fact that the inter-precipitate spacing is so small (~100 nm) that a higher stress level must be reached before Orowan loops can become active (Fig. 3).

In summary, we present two new Fe–Mn steels with a low-carbon martensitic matrix and elements for the formation of precipitates (Ni, Ti, Al, Mo). One alloy had up to 15 vol.% of retained austenite (12 wt.% Mn, maraging TRIP steel), while the other had no retained austenite after quenching (9 wt.% Mn, maraging steel). Both materials revealed a significant increase in both strength and total elongation after aging heat treatment. The unexpected increase in elongation was attributed to the formation of nanoscaled precipitates leading to an Orowan hardening mechanism at intermediate strains.

[1] J. Inoue, S. Nambu, Y. Ishimoto, T. Koseki, Scripta Mater. 59 (2008) 1055.
[2] S. Nambu, M. Michiuchi, Y. Ishimoto, K. Asakura, J. Inoue, T. Koseki, Scripta Mater. 59 (2008) 1055.
[3] J.R. Patel, M. Cohen, Acta Metall. 1 (1953) 531.
[4] H.K.D.H. Bhadeshia, D.V. Edmonds, Metall. Trans. 10A (1979) 895.
[5] M. Takahashi, H.K.D.H. Bhadeshia, Mater. Trans. JIM 32 (1991) 689–696.
[6] P.J. Jacques, E. Girault, T. Catlin, N. Geerlofs, T. Kop, S. van der Zwaag, F. Delannay, Mater. Sci. Eng. A 273–275 (1999) 475.
[7] M. De Meyer, D. Vanderschueren, B.C. De Cooman, ISIJ. Int. 39 (1999) 813.
[8] S. Traint, A. Pichler, K. Hauzenberger, P. Stiaszny, E. Werner, Steel Res. Int. 73 (2002) 259.
[9] P.J. Jacques, Curr. Opin. Solid State Mater. Sc. 8 (2004) 59.
[10] S. Zaefferer, J. Ohlert, W. Bleck, Acta Mater. 52 (2004) 2765.
[11] R.F. Decker, J.T. Eash, A.J. Goldman, Trans. ASM 55 (1962) 58.
[12] R.F. Decker (Ed.), Source Book on Maraging Steels, ASM International, Metals Park, OH, 1979.
[13] W. Sha, A. Cerezo, G.D.W. Smith, Metall. Trans. 24A (1993) 1251.
[14] V.K. Vasudervan, S.J. Kim, C.M. Wayman, Metall. Trans. 21A (1990) 2655.
[15] C. Servant, N. Bouzid, Acta Metall. 36 (1988) 2771.
[16] R. Tewari, S. Majumder, I.S. Batra, G.K. Dey, S. Banerjee, Acta Mater. 48 (2000) 1187.
[17] S. Hossein Nedjad, M.R. Movaghar Garabagh, M. Nili Ahmadabadi, H. Shirazi, Mater. Sci. Eng. A 473 (2008) 249.
[18] G.P. Miller, W.I. Mitchell, J. Iron Steel Inst. 20 (1965) 899.
[19] R. Kapoor, I.S. Batra, Mater. Sci. Eng. A 371 (2004) 324.